Published in final edited form as:
J Theor Biol. 2013 January 7; 316C: 42–48. doi:10.1016/j.jtbi.2012.09.029.

Mechanical Buckling of Arterioles in Collateral Development

Qin Liu and **Hai-Chao Han**
Department of Mechanical Engineering, University of Texas at San Antonio

Abstract

Collateral arterioles enlarge in both diameter and length, and develop corkscrew-like tortuous patterns during remodeling. Recent studies showed that artery buckling could lead to tortuosity. The objective of this study was to determine arteriole critical buckling pressure and buckling pattern during arteriole remodeling. Arterioles were modeled as elastic cylindrical vessels with an elastic matrix support and underwent axial and radial growth. Our results demonstrated that arteriole critical buckling pressure decreased with increasing axial growth ratio and radius growth ratio, but increased with increasing wall thickness. Arteriole buckling mode number increased (wave length decreased) with increasing axial growth ratio, but decreased with increasing radius growth ratio and wall thickness. Our study suggests that axial growth in arterioles makes them prone to buckling and that buckling leads to tortuous collaterals. These results shed light on the mechanism of collateral arteriole tortuosity.

Keywords

arteriole buckling; tortuosity; critical pressure; remodeling; axial growth ratio; radius growth ratio; artery; modeling

1. Introduction

Vessel tortuosity often occurs during arteriogenesis, the growth of preexisting arterioles. Arterioles develop into tortuous collateral arteries after occlusion of a major artery. “Corkscrew” collaterals have been reported in coronary and peripheral arteries (Schaper and Buschmann 1999; Cai et al. 2003; Shireman and Quinones 2005). Tortuosity increases the flow resistance in collateral arterioles (Heil and Schaper 2004; Eitenmuller et al. 2006). Tortuosity may also activate platelets and consequently induce thrombosis in microvessels (Liu et al. 2008; Chesnutt and Han 2011). On the other hand, an increase in capillary tortuosity could increase the interface area of capillary to tissue, thus promoting muscle tissue oxygenation (Goldman and Popel 2000; Charifi et al. 2004). Arterioles around tumor cells often develop tortuous shapes, and the tortuosity level has been associated with the malignancy of tumors (Bullitt et al. 2005; Pries et al. 2009; Vakoc et al. 2009). Therefore, it is important to understand the relationship between microvessel development and tortuosity.

Address for Correspondence: Dr. Hai-Chao Han, Department of Mechanical Engineering, The University of Texas at San Antonio, San Antonio, TX 78249, Tel: (210) 458-4952, Fax: (210) 458-6504, haichao.han@utsa.edu.

Conflict of interest statement
The authors have no conflict of interest.

Tortuous vessels are also often observed in medium to large arteries and veins in humans and animals (Han 2012), and are often associated with hypertension, aging, and atherosclerosis (Smedby and Bergstrand 1996; Del Corso et al. 1998; Pancera et al. 2000; Hiroki et al. 2002; Thore et al. 2007; Han 2012). Genetic defects and other pathologic changes such as degenerative vascular diseases have also been linked to artery tortuosity (Dobrin et al. 1988; Wagenseil et al. 2005; Callewaert et al. 2008). While it is speculated that arterial growth may lead to tortuosity, the physical mechanisms and the quantitative relation remain unclear.

Collateral arteriole growth begins with a rapid onset of proliferation leading to outward remodeling in seven days after the occlusion, which is followed by extensive remodeling (Ito et al. 1997). During the development of collateral arterioles, smaller vessels regress, and larger ones increase in diameter. However, the enlargement in diameter is often limited. In optimal conditions, 35 – 40% of the maximal flow can be recovered by collateral arteries (Lazarous et al. 1996; Ito et al. 1997). Though creating an arterio-venous shunt may completely restore the maximal collateral flow (Eitenmuller et al. 2006), it is hard to achieve clinically. One possible reason for the incomplete recovery of blood flow could be the tortuosity of collateral arterioles. However, how tortuosity is generated in collateral arterioles and its relationship to arteriole remodeling remain unclear.

Recent studies have shown that arteries may lose stability and buckle when their lumen pressure is elevated or axial tension is reduced (Han 2007; Han 2009; Lee et al. 2012). Artery buckling causes arteries to deform into tortuous shapes, starting with a small lateral deflection and developing into a large deflection if the pressure continues to increase. *In vivo* experiments showed that rabbit carotid arteries under reduced axial tension adapted over time and became permanently tortuous (Jackson et al. 2005), suggesting that buckling could lead to tortuosity. However, the effects of growth on arterial mechanical stability and buckling behavior have not been investigated.

Therefore, the objective of this study was to determine arteriole critical buckling pressure and buckling pattern change due to axial and radial growth and remodeling using model simulations.

2. Methods

2.1. Buckling equation

Arterioles were modeled as nonlinear elastic circular cylinders surrounded by soft tissues. The tissues were modeled as linear elastic matrices. Accordingly, arteriole buckling pressure p_{cr} was determined using the artery buckling equation given by (Han 2009):

$$p_{cr}=\frac{N}{\pi R_i^2}+\frac{EI}{\pi R_i^2}\left(\frac{n\pi}{l}\right)^2+\frac{k_s}{\pi R_i^2}\left(\frac{l}{n\pi}\right)^2 \quad (1)$$

where N is the axial force, R_i is the lumen radius, EI is the cross sectional bending rigidity, k_s is the Young's modulus of the surrounding matrix, l is the vessel length, and n is the buckling wave mode number. N was determined by the transmural pressure p and the strain. The bending rigidity EI is a function of arteriole cross sectional dimensions and the strain components as given in detail previously (see appendix in (Han 2011)). EI is also affected by the lumen pressure and axial stretch ratio since the strain components are functions of pressure and axial stretch ratio. The critical pressure p_{cr} of an arteriole with given R_i, l, and k_s, was determined following the iteration steps decreased previously (Han 2009). Briefly, for each assumed wave number n, the buckling pressure was determined through iterations using Equation 1. The process was repeated for a range of n values (>1. The corresponding

p_{cr} value first decreases and then increases with increasing n). The actual critical buckling pressure was determined by finding the n value that gave the minimum p_{cr} value (Han 2009).

2.2. Determination of arteriole wall material constants

The mechanical behavior of arteriolar walls was characterized by Fung's exponential strain energy function (Fung 1993):

$$w=\frac{1}{2}b_0e^Q+K[(1+2E_r)(1+2E_\theta)(1+2E_z)-1]$$
$$Q=b_1E_\theta^2+b_2E_z^2+b_3E_r^2+2b_4E_\theta E_z+2b_5E_zE_r+2b_6E_rE_\theta \quad (2)$$

where $b_0 - b_6$ are the material constants, and K is a Lagrangian multiplier for incompressibility. E_θ, E_z, and E_r are the Green strain components in the circumferential, axial, and radial directions, which all refer to the zero-stress state. By solving the equilibrium equation for a cylindrical arteriole under axial load and internal pressure, the internal pressure p and axial force N in the vessel were expressed as (Fung 1990; Humphrey 2002; Han 2008; Han 2009):

$$p=\int_{Ri}^{Re}[(1+2E_\theta)(b_1E_\theta+b_4E_z+b_6E_r)-(1+2E_r)(b_6E_\theta+b_5E_z+b_3E_r)]b_0e^Q\frac{d\xi}{\xi}$$
$$N=\pi R_i^2\,p+\pi\int_{Ri}^{Re}[2(1+2E_z)(b_4E_\theta+b_2E_z+b_5E_r)-(1+2E_r)(b_6E_\theta+b_5E_z+b_3E_r)-(1+2E_\theta)(b_1E_\theta+b_4E_z+b_6E_r)]b_0e^Q r dr \quad (3)$$

wherein R_i and R_e are the inner and outer radii, respectively. The material constants $b_0 - b_6$ were determined by fitting Eq. (3) to a previously reported pressure-diameter relation of cat mesenteric arterioles incorporating the initial dimensions (outer/inner radius and wall thickness t) (Gore 1974). Residual strain was not measured in this previous study (Gore 1974). However, since our previous studies have shown that residual strain (opening angle) had little effect on the critical pressure (Han 2009; Liu and Han 2012), the residual strain in the arteriole was neglected in current simulations (opening angle = 180°). We also assumed that the arterioles were free to expand in the mesentery, and thus the axial force was $N = \pi r^2 p$. Using a custom code in Matlab (Lee et al. 2012; Liu and Han 2012), we obtained b_1 = 2.0, b_2 = 0.001, b_3 = 2.0, b_4 = 0.2555, b_5 = 0.001, b_6 = 1.996, and b_0 = 38.949 kPa.

2.3. Arteriole parameters and simulation conditions

In our simulations, arteriole length l was assumed to be 10 mm, with the initial lumen radius R_i = 50 μm and outer radius R_e = 60 μm. The arteriole was pre-stretched axially at a stretch ratio of 1.5. The stiffness of supporting matrix was k_s = 5 kPa, unless otherwise specified.

To describe the growth of arterioles, we defined growth ratio as the percentage of dimension change due to growth from the original length under no-load condition. Collateral arterioles elongate while enlarging radially (outward remodeling). So we examined arterioles with combinations of axial growth ratios and radial growth ratios. The axial growth ratios were examined in the range of 0 to 30% (Herzog et al. 2002). Since arteriolar wall cross section area might decrease (hypotrophic), increase (hypertrophic), or remain the same (eutrophic) (Mulvany 1999), both lumen diameter and wall thickness (thus the outer diameter) changes were examined. The lumen diameter and wall thickness were assumed to increase up to 2-fold and 2.5-fold, respectively, following a previous experimental observation (Herzog et al. 2002).

Arteriole buckling was simulated first for axial growth alone and then for combined axial and radial growth.

3. Results

3.1. Effect of axial growth on arteriole critical buckling

Simulations showed that axial growth of arterioles reduced the critical buckling pressure. For an arteriole (R_i = 50 μm, t = 10 μm, and l = 10mm) within a surrounding matrix of stiffness k_s = 5 kPa, when the axial growth ratio increased from 0 to 30% while the lumen radius and wall thickness remained unchanged, the critical buckling pressure decreased from 51.0 to 22.2 mmHg (■, Fig. 1a). Accordingly, the buckling wave mode number increased from the 23rd to the 33rd mode (■, Fig. 1b). The wave length decreased from 435 to 303 μm. These results indicate that at a higher axial growth ratio the arteriole more easily buckled and became more tortuous. Figure 1c illustrates the first seven wave mode shapes for arteriole buckling.

3.2. Effect of supporting tissue stiffness on arteriole critical buckling

The stiffness of the surrounding matrix affects the critical buckling pressure and buckling mode. Arterioles without supporting tissue (k_s = 0) buckle into the base mode (n = 1) under increasing lumen pressure. However, with supporting tissue (k_s = 0.5, 1 and 5 kPa), arterioles buckled into higher order mode shapes (Fig. 1b) and at higher critical pressures (Fig. 1a). Stronger supporting tissue (k_s = 5) led to higher critical buckling pressures and higher wave shape modes in arterioles with the same axial growth ratio. For example, for the arteriole with the lumen radius 50 μm, wall thickness 10 μm, and length 10 mm, at axial growth ratio 10%, the critical buckling pressures were 15.3, 18.9, and 38.2 mmHg, and the corresponding wave modes were 18, 20, and 26 for k_s = 0.5, 1, and 5 kPa, respectively.

3.3. Effect of arteriole radius growth on critical buckling

Radius growth of arterioles also reduced the critical pressure. For an arteriole maintaining a constant thickness, both the critical pressure and buckling wave number decreased with increasing radius growth ratio (Fig. 2). For example, at a given wall thickness t = 20 μm and axial growth ratio 10%, when arteriolar radius growth ratio increased from 0 to 3 (an increase of radius from 50 to 200 μm), the critical pressure p_{cr} decreased from 52.8 to 29.3 mmHg, and buckling wave mode number changed from 23rd to 7th.

In addition, for a given radius growth ratio and axial growth ratio, the growth in wall thickness increased the critical pressure (Fig. 3a) and reduced the buckling wave mode number (Fig. 3b). For example, at a given lumen radius growth ratio of 2 (R_i = 100 μm) and axial growth ratio of 10%, with the increase of wall thickness from 10 to 40 μm, the critical buckling pressure increased from 29.3 to 52.8 mmHg and the corresponding buckling wave mode number decreased from 14th to 11th.

Having noticed the same critical pressure (52.8 mmHg) for the two vessels of the same wall thickness to radius ratio (but different thickness and radius), we further analyzed the effect of arteriole dimensions on the critical pressure. Our results demonstrated that the final remodeled wall thickness to lumen radius ratio t/R_i was a determinate parameter for the critical buckling pressure, though not the buckling mode shape (Fig. 4). Table 1 illustrates t/R_i values and types of remodeling at various changes in R_i and R_e, as well as the corresponding wave modes. It is seen that the change of wave mode with t/R_i value was not monotonic but biphasic.

3.4. Effect of wall material property changes on critical buckling

To mimic the changes in material properties of collateral arteriolar walls, we considered the changes in material constant b_0, which directly reflects the stiffness of arteries at all strain levels. Our results demonstrated that elevation of material stiffness increased the critical

buckling pressures (Fig. 5). For example, at the same axial growth ratio of 10%, when the value of b_0 (38.95 kPa) decreased to $0.5b_0$ (19.47 kPa) or increased to $2b_0$ (77.90 kPa), the critical pressure decreased to 30.9 mmHg or increased to 61.5 mmHg, respectively (Fig. 5a), and the corresponding buckling wave mode increased from 12^{th} to 14^{th}, or remained unchanged 12^{th}, respectively (Fig. 5b).

4. Discussion

This study illustrated the relation between collateral arteriole growth/remodeling and mechanical buckling. Our results showed that arteriolar axial growth reduced the critical buckling pressure, making arterioles prone to buckling and consequently leading to tortuous collaterals. In addition, radius growth at a given wall thickness reduced the critical pressure, and wall thickening at a given radius elevated the critical pressure.

4.1 Effects of dimensional growth on critical pressure

The effects of dimensional growth on the critical buckling pressure can be explained using a buckling equation, which illustrated that arterial buckling pressure decreased with reduced axial stretch ratio and wall thickness to radius ratio (Han 2007; Han 2008; Han 2009).

First, axial growth reduced the axial stretch ratio of the arteriole since the distance between the up- and down-stream branching points of a collateral arteriole was restricted by the anatomic positions. Therefore, an arteriole with a higher axial growth ratio would have a lower stretch ratio and thus a lower critical buckling pressure. These results are consistent with the conclusion that the reduction of axial tension in rabbit carotid arteries led to tortuous arteries in a previous *in vivo* study (Jackson et al. 2005). The study also showed that the reduction of axial tension elevated the proliferation rates of both endothelial cells and smooth muscle cells. These results indicated that reduced axial tension may stimulate arteriole growth and remodeling, and suggested a possible dynamic feedback mechanism that needs to be investigated in the future.

Second, increasing arteriole radius at a given wall thickness reduced the wall thickness to radius ratio and thus reduced the critical buckling pressure making arterioles prone to buckling. Although the change of critical pressure with lumen radius is biphasic in general (Han 2007; Datir 2010), the critical pressure reduced monotonically in the radius growth range discussed (from 50 to 200 μm) for arterioles. On the other hand, wall thickening at a given radius increased the critical pressure. However, when arteriolar lumen radius and outer radius both increased at the same ratio, the wall thickness to radius ratio remained the same and the critical buckling pressure did not change. The critical buckling pressure increased only when the wall thickness increased at a higher ratio than the lumen radius did, *i.e.*, when the ratio of wall thickness to lumen radius (t/R_i) increased. These results demonstrated that the determining parameter was the final wall thickness to lumen radius ratio, not the wall thickness per se (Han 2007; Han 2008; Han 2009).

One interesting finding of this study is that the radial growth of an arteriole alone, without any axial length change or wall thickening, would reduce the critical buckling pressure. Collateral arterioles both enlarge their diameters and elongate their lengths during remodeling. These combined radius and axial growths intensify the reduction in critical pressure. Thus collateral arterioles are very often seen to be tortuous.

4.2. Determination of matrix stiffness k_S

Arterioles were surrounded by supporting tissue. Our simulation presumed that collateral arterioles did not buckle at the beginning of the remodeling, where the critical buckling pressure should be above the lumen pressure in the arterioles. After remodeling started, with

the axial and/or radial growth, arterioles could buckle. The lumen pressure measured in collaterals after the ligation of the femoral artery was 30 – 40 mmHg (Chen et al. 1994; Unthank et al. 1995; Unthank et al. 1996). Therefore, a matrix stiffness k_s = 5 kPa was used in the simulations so that the estimated critical buckling pressure (51.0 mmHg) of the arteriole was above the normal pressure. The critical buckling pressure dropped below the normal pressure at various axial and radius growth ratios. While further studies are needed to determine the actual stiffness that may vary depending on the surrounding matrix, we expect that the trend demonstrated by our simulation will remain similar.

4.3. Estimation of buckling wave mode number

The non-monotonic change of buckling wave modes with t/R_i ratio could be explained using the theoretical equation for buckling wave mode number n (Han 2009)

$$n^2(n+1)^2=\frac{k_s}{EI}\left(\frac{l}{\pi}\right)^4 \quad (4)$$

Approximating $I = \pi R^3 t$ for cylindrical arterioles and assuming E is a constant yield

$$n \approx \frac{l}{\pi R_i}\sqrt[4]{\frac{k_s}{E\pi}}\sqrt[4]{\frac{1}{t/R_i}} \quad (5)$$

It is seen that wave mode number n is not determined by t/R_i ratio alone but by both t and R_i. For arterioles with constant thickness t, the wave mode number decreased with the increase of R_i (decrease of t/R_i). For arterioles with constant R_i, the wave mode number decreased with the increase of t (increase of t/R_i).

4.4. Model limitations

A limitation of current study is that the supporting tissue was assumed to be linear elastic. The linear elastic matrix assumption was used due to its simplicity and to be consistent with our previous study (Han 2009). Since arterioles had very small lateral deflection when buckling occurred initially, the reaction force generated by the matrix could be assumed to be linearly related to the deflection. Thus, the linear elastic matrix assumption was reasonable. In addition, the comparison of the critical buckling of arterioles at different axial and radial growth ratios was done for linear elastic matrix of the same stiffness. So we expected that the linear elastic matrix assumption did not affect the overall conclusion.

Another assumption was that arteriole growth was axially and circumferentially uniform. The newly-grown parts did not change the uniformity of the whole vessel. Even though previous simulation results showed that geometric variations could slightly reduce or increase the buckling pressure (Datir 2010), the effects of these imperfections were expected to be small.

Our simulations showed that changes in the mechanical properties affect the critical pressure and wave mode. However, it is unclear how changes in mechanical properties of the arteriole wall are associated with axial growth or radial growth. A previous study demonstrated that the stiffness of arterioles increased ~25% during the development of diabetes (Liu and Fung 1992). Our simulations showed that a 2-fold increase in stiffness (b_0) increased p_{cr} by ~50% at each axial growth ratio, and a 25% increase in stiffness might only increase p_{cr} by approximately 2 – 3 mmHg. Further studies are needed to experimentally measure the material properties of collateral arterioles during the remodeling process.

4.5. Clinical relevance

Collateral arterioles expand in diameter to increase blood flow to the ischemic tissue after a main artery is occluded. The increased flow increases fluid shear stress, which has been considered as a trigger for collateral growth through a complex signaling process involving monocyte chemotactic protein-1 (MCP-1), angiotension, vascular endothelial growth factor, which results in increased monocyte deposition, cell proliferation, and matrix metalloproteinase activities (Ito et al. 1997; Shireman 2007; van Royen et al. 2009). Growth of collateral arterioles could result in axial growth (elongation), which reduces the axial tension in the arterioles and often makes collateral arterioles tortuous. Reduction in axial tension could further stimulate cell proliferation and generate tortuosity (Jackson et al. 2005; Lee et al. 2012). However, the maximal flow can only be partially recovered by collateral arterioles (Lazarous et al. 1996). One possible reason is the increase of flow resistance due to the development of tortuosity in collateral arterioles (Heil and Schaper 2004; Eitenmuller et al. 2006). Although the molecular mechanisms that stimulate and regulate arteriole growth still remain to be investigated, the current model helps us to understand the formation of the tortuous shape in the process. Our results also suggest that raising the critical buckling pressure of the arteriole, by changing the wall material property (stiffening the wall) or stiffening the supporting matrix, will make the arteriole more stable. This is consistent with previous reports that showed enhancing tissue support would prevent vessel tortuosity (Lu et al. 1993; Han et al. 1998; Hamza et al. 2003). Our study sheds new light on the mechanism of the development of tortuous collaterals.

On the other hand, buckling of arterioles could be beneficial. For people with α–thalassemia disease where more muscle tissue oxygenation is wanted (Vincent et al. 2010), increasing capillary tortuosity may increase the contact area of capillaries to tissue (Goldman and Popel 2000; Charifi et al. 2004). Factors that reduce the critical buckling pressure in the capillary would be potential targets for treatment.

In conclusion, growth and remodeling in arterioles can lead to mechanical buckling. Arteriole buckling pressure decreases with axial growth, but increases with increasing wall thickness to lumen radius ratio. Arteriolar buckling mode number increases with axial growth, but decreases with increasing radius and wall thickness. Collateral arterioles become prone to buckling with growth in radius and axial length, which could be a mechanism for the development of tortuous collaterals.

Understanding the mechanisms of tortuosity initiation and development in the microvasculature has wide implications in vascular physiology and pathology, as well as in tissue regeneration. This understanding will help us to develop new approaches for the prevention and treatment (reduction or augmentation) of arteriolar tortuosity.

Acknowledgments

This work was supported by CAREER award #0644646 from the National Science Foundation and grant R01HL095852 from the National Institutes of Health.

References

Bullitt E, Zeng D, Gerig G, Aylward S, Joshi S, Smith JK, Lin W, Ewend MG. Vessel tortuosity and brain tumor malignancy: A blinded study. Acad Radiol. 2005; 12(10):1232–40. [PubMed: 16179200]

Cai WJ, Koltai S, Kocsis E, Scholz D, Kostin S, Luo X, Schaper W, Schaper J. Remodeling of the adventitia during coronary arteriogenesis. Am J Physiol Heart Circ Physiol. 2003; 284(1):H31–40. [PubMed: 12388238]

Callewaert BL, Willaert A, Kerstjens-Frederikse WS, De Backer J, Devriendt K, Albrecht B, Ramos-Arroyo MA, Doco-Fenzy M, Hennekam RC, Pyeritz RE, Krogmann ON, Gillessen-kaesbach G, Wakeling EL, Nik-zainal S, Francannet C, Mauran P, Booth C, Barrow M, Dekens R, Loeys BL, Coucke PJ, De Paepe AM. Arterial tortuosity syndrome: Clinical and molecular findings in 12 newly identified families. Hum Mutat. 2008; 29(1):150–8. [PubMed: 17935213]

Charifi N, Kadi F, Feasson L, Costes F, Geyssant A, Denis C. Enhancement of microvessel tortuosity in the vastus lateralis muscle of old men in response to endurance training. J Physiol. 2004; 554(Pt 2):559–69. [PubMed: 14578492]

Chen DS, Gu YD, Su YC. [distal blood pressure changes after ligation of the femoral artery or vein in the rat]. Zhonghua Wai Ke Za Zhi. 1994; 32(6):374–5. [PubMed: 7842966]

Chesnutt JK, Han HC. Tortuosity triggers platelet activation and thrombus formation in microvessels. J Biomech Eng. 2011; 133(12):121004. [PubMed: 22206421]

Datir P, Lee AY, Lamm SD, Han HC. Effect of geometric variations on the vuckling of arteries. Int J Appl Mech. 2010; 3(2):385–406. [PubMed: 22287983]

Del Corso L, Moruzzo D, Conte B, Agelli M, Romanelli AM, Pastine F, Protti M, Pentimone F, Baggiani G. Tortuosity, kinking, and coiling of the carotid artery: Expression of atherosclerosis or aging? Angiology. 1998; 49(5):361–71. [PubMed: 9591528]

Dobrin PB, Schwarcz TH, Baker WH. Mechanisms of arterial and aneurysmal tortuosity. Surgery. 1988; 104(3):568–71. [PubMed: 3413685]

Eitenmuller I, Volger O, Kluge A, Troidl K, Barancik M, Cai WJ, Heil M, Pipp F, Fischer S, Horrevoets AJ, Schmitz-Rixen T, Schaper W. The range of adaptation by collateral vessels after femoral artery occlusion. Circ Res. 2006; 99(6):656–62. [PubMed: 16931799]

Fung, YC. Biomechanics: Motion, flow, stress, and growth. New York: Springer-Verlag; 1990.

Fung, YC. Biomechanics: Mechanical properties of living tissues. New York: Springer-Verlag; 1993.

Goldman D, Popel AS. A computational study of the effect of capillary network anastomoses and tortuosity on oxygen transport. J Theor Biol. 2000; 206(2):181–94. [PubMed: 10966756]

Gore RW. Pressures in cat mesenteric arterioles and capillaries during changes in systemic arterial blood pressure. Circ Res. 1974; 34(4):581–91. [PubMed: 4826932]

Hamza LH, Dang Q, Lu X, Mian A, Molloi S, Kassab GS. Effect of passive myocardium on the compliance of porcine coronary arteries. Am J Physiol Heart Circ Physiol. 2003; 285(2):H653–60. [PubMed: 12860566]

Han HC. A biomechanical model of artery buckling. J Biomech. 2007; 40(16):3672–8. [PubMed: 17689541]

Han HC. Nonlinear buckling of blood vessels: A theoretical study. J Biomech. 2008; 41(12):2708–13. [PubMed: 18653191]

Han HC. Blood vessel buckling within soft surrounding tissue generates tortuosity. J Biomech. 2009; 42(16):2797–801. [PubMed: 19758591]

Han HC. Determination of the critical buckling pressure of blood vessels using the energy approach. Ann Biomed Eng. 2011; 39(3):1032–40. [PubMed: 21116846]

Han HC. Twisted blood vessels: Symptoms, etiology and biomechanical mechanisms. J Vasc Res. 2012; 49(3):185–197. [PubMed: 22433458]

Han HC, Zhao L, Huang M, Hou LS, Huang YT, Kuang ZB. Postsurgical changes of the opening angle of canine autogenous vein graft. J Biomech Eng. 1998; 120(2):211–6. [PubMed: 10412382]

Heil M, Schaper W. Influence of mechanical, cellular, and molecular factors on collateral artery growth (arteriogenesis). Circ Res. 2004; 95(5):449–58. [PubMed: 15345667]

Herzog S, Sager H, Khmelevski E, Deylig A, Ito WD. Collateral arteries grow from preexisting anastomoses in the rat hindlimb. Am J Physiol Heart Circ Physiol. 2002; 283(5):H2012–20. [PubMed: 12384480]

Hiroki M, Miyashita K, Oda M. Tortuosity of the white matter medullary arterioles is related to the severity of hypertension. Cerebrovasc Dis. 2002; 13(4):242–50. [PubMed: 12011548]

Humphrey, JD. Cardiovascular solid mechanics: Cells, tissues, and organs. New York: Springer; 2002.

Ito WD, Arras M, Winkler B, Scholz D, Schaper J, Schaper W. Monocyte chemotactic protein-1 increases collateral and peripheral conductance after femoral artery occlusion. Circ Res. 1997; 80(6):829–37. [PubMed: 9168785]

Jackson ZS, Dajnowiec D, Gotlieb AI, Langille BL. Partial off-loading of longitudinal tension induces arterial tortuosity. Arterioscler Thromb Vasc Biol. 2005; 25(5):957–62. [PubMed: 15746437]

Lazarous DF, Shou M, Scheinowitz M, Hodge E, Thirumurti V, Kitsiou AN, Stiber JA, Lobo AD, Hunsberger S, Guetta E, Epstein SE, Unger EF. Comparative effects of basic fibroblast growth factor and vascular endothelial growth factor on coronary collateral development and the arterial response to injury. Circulation. 1996; 94(5):1074–82. [PubMed: 8790049]

Lee AY, Han B, Lamm SD, Fierro CA, Han HC. Effects of elastin degradation and surrounding matrix support on artery stability. Am J Physiol Heart Circ Physiol. 2012; 302(4):H873–84. [PubMed: 22159998]

Liu Q, Han HC. Mechanical buckling of artery under pulsatile pressure. J Biomech. 2012; 45(7):1192–8. [PubMed: 22356844]

Liu Q, Mirc D, Fu BM. Mechanical mechanisms of thrombosis in intact bent microvessels of rat mesentery. J Biomech. 2008; 41(12):2726–34. [PubMed: 18656200]

Liu SQ, Fung YC. Influence of stz-induced diabetes on zero-stress states of rat pulmonary and systemic arteries. Diabetes. 1992; 41(2):136–46. [PubMed: 1733801]

Lu Y, Huang Y, Zhao L, Li R, Shi K, Ma P, Chu X. Management of major arterial injuries of limbs: A study of 166 cases. Cardiovasc Surg. 1993; 1(5):486–8. [PubMed: 8076082]

Mulvany MJ. Vascular remodelling of resistance vessels: Can we define this? Cardiovasc Res. 1999; 41(1):9–13. [PubMed: 10325946]

Pancera P, Ribul M, Presciuttini B, Lechi A. Prevalence of carotid artery kinking in 590 consecutive subjects evaluated by echocolordoppler. Is there a correlation with arterial hypertension? J Intern Med. 2000; 248(1):7–12. [PubMed: 10947875]

Pries AR, Cornelissen AJ, Sloot AA, Hinkeldey M, Dreher MR, Hopfner M, Dewhirst MW, Secomb TW. Structural adaptation and heterogeneity of normal and tumor microvascular networks. PLoS Comput Biol. 2009; 5(5):e1000394. [PubMed: 19478883]

Schaper W, Buschmann I. Arteriogenesis, the good and bad of it. Eur Heart J. 1999; 20(18):1297–9. [PubMed: 10462463]

Shireman PK. The chemokine system in arteriogenesis and hind limb ischemia. J Vasc Surg. 2007; 45(Suppl A):A48–56. [PubMed: 17544024]

Shireman PK, Quinones MP. Differential necrosis despite similar perfusion in mouse strains after ischemia. J Surg Res. 2005; 129(2):242–50. [PubMed: 16051277]

Smedby O, Bergstrand L. Tortuosity and atherosclerosis in the femoral artery: What is cause and what is effect? Ann Biomed Eng. 1996; 24(4):474–80. [PubMed: 8841722]

Thore CR, Anstrom JA, Moody DM, Challa VR, Marion MC, Brown WR. Morphometric analysis of arteriolar tortuosity in human cerebral white matter of preterm, young, and aged subjects. J Neuropathol Exp Neurol. 2007; 66(5):337–45. [PubMed: 17483690]

Unthank JL, Nixon JC, Burkhart HM, Fath SW, Dalsing MC. Early collateral and microvascular adaptations to intestinal artery occlusion in rat. Am J Physiol. 1996; 271(3 Pt 2):H914–23. [PubMed: 8853325]

Unthank JL, Nixon JC, Lash JM. Early adaptations in collateral and microvascular resistances after ligation of the rat femoral artery. J Appl Physiol. 1995; 79(1):73–82. [PubMed: 7559251]

Vakoc BJ, Lanning RM, Tyrrell JA, Padera TP, Bartlett LA, Stylianopoulos T, Munn LL, Tearney GJ, Fukumura D, Jain RK, Bouma BE. Three-dimensional microscopy of the tumor microenvironment in vivo using optical frequency domain imaging. Nat Med. 2009; 15(10):1219–23. [PubMed: 19749772]

van Royen N, Piek JJ, Schaper W, Fulton WF. A critical review of clinical arteriogenesis research. J Am Coll Cardiol. 2009; 55(1):17–25. [PubMed: 20117358]

Vincent L, Feasson L, Oyono-Enguelle S, Banimbek V, Denis C, Guarneri C, Aufradet E, Monchanin G, Martin C, Gozal D, Dohbobga M, Wouassi D, Garet M, Thiriet P, Messonnier L. Remodeling of skeletal muscle microvasculature in sickle cell trait and alpha-thalassemia. Am J Physiol Heart Circ Physiol. 2010; 298(2):H375–84. [PubMed: 19915173]

Wagenseil JE, Nerurkar NL, Knutsen RH, Okamoto RJ, Li DY, Mecham RP. Effects of elastin haploinsufficiency on the mechanical behavior of mouse arteries. Am J Physiol Heart Circ Physiol. 2005; 289(3):H1209–17. [PubMed: 15863465]

Highlights

- We modeled arteriole buckling behavior associated with growth and remodeling
- Arteriole length growth decreases the buckling pressure and buckling wave length
- Radius growth decreases the buckling pressure but increases buckling wave length
- Increasing wall thickness increases the buckling pressure and buckling wave length
- Adaptive growth makes arterioles prone to buckling & leads to tortuous collaterals

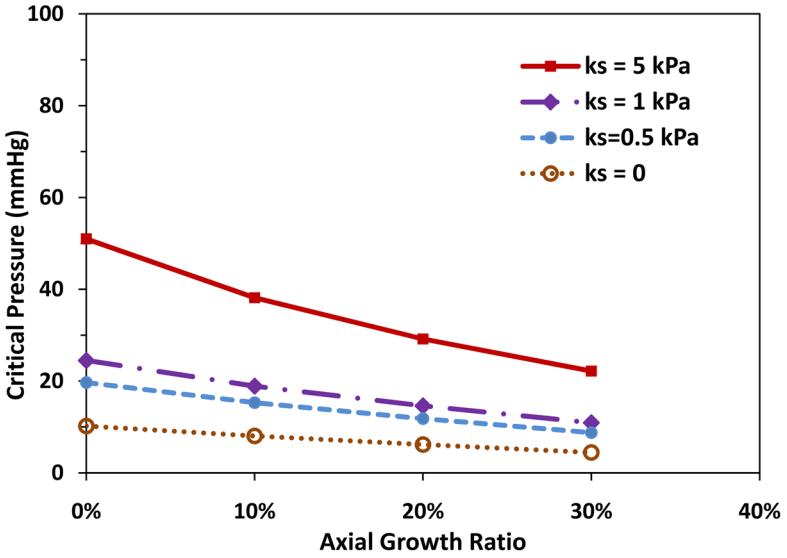

(a)

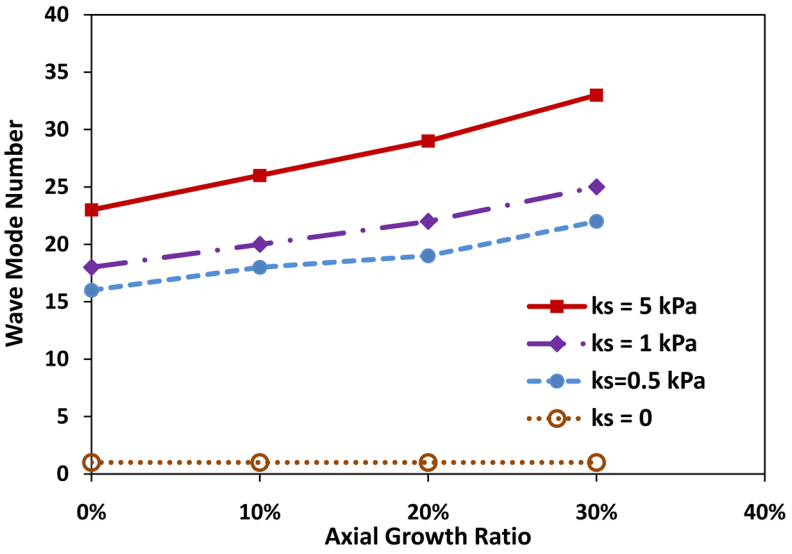

(b)

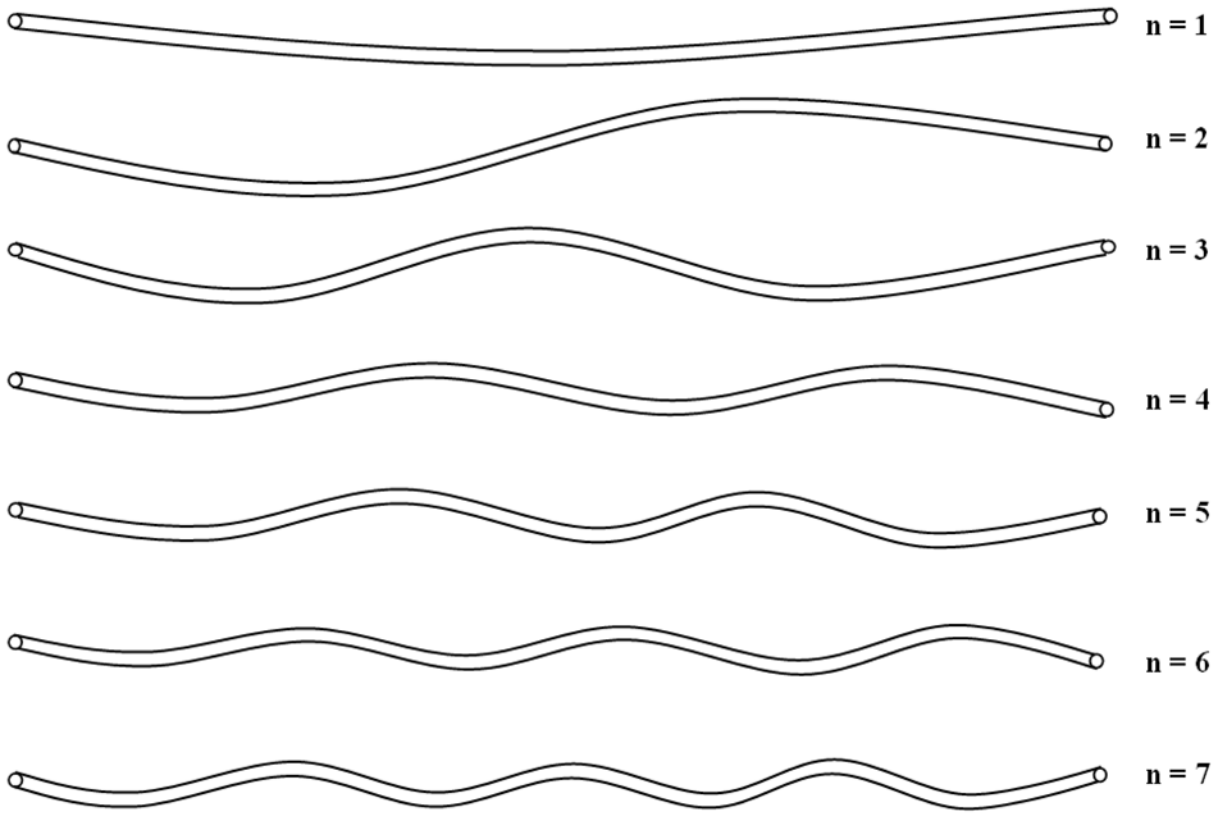

(c)

Figure 1.
Critical buckling pressure (a) and buckling mode (b) plotted as functions of axial growth ratio at different matrix stiffness. The lumen radius R_i, wall thickness t, and length of the collateral arteriole l were 50 μm, 10 μm, and 10 mm respectively. (c) Illustration of buckling wave mode shapes.

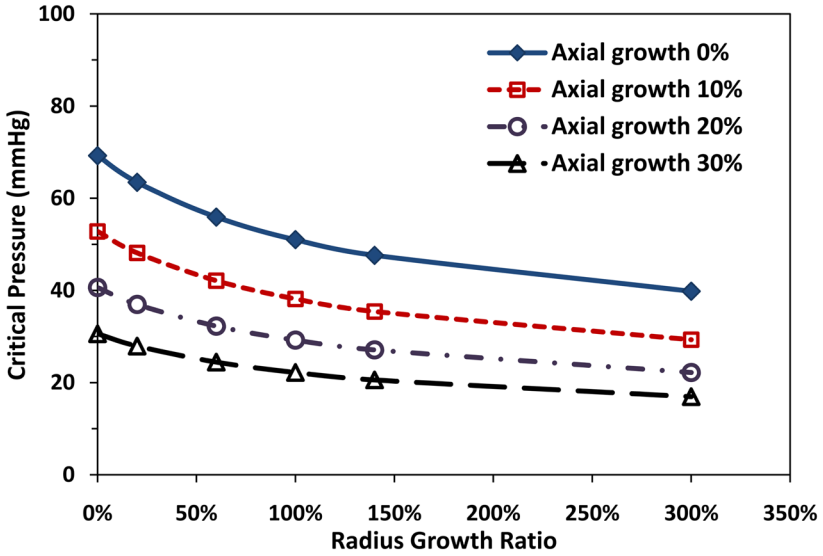

(a)

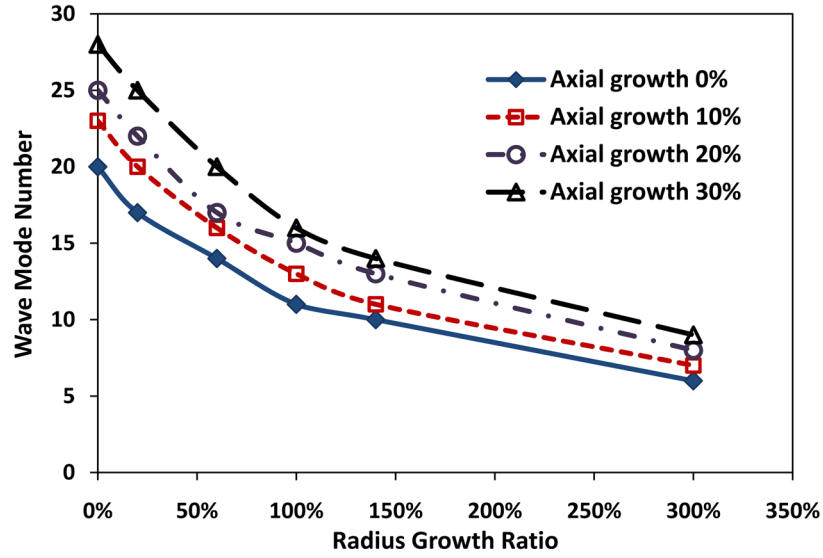

(b)

Figure 2.

Critical buckling pressure (a) and buckling mode (b) plotted as functions of arteriolar radius growth ratio at a constant wall thickness (t = 20 μm). Arteriole initial length l = 10 mm, initial lumen radius R_i = 50 μm, and k_s = 5 kPa.

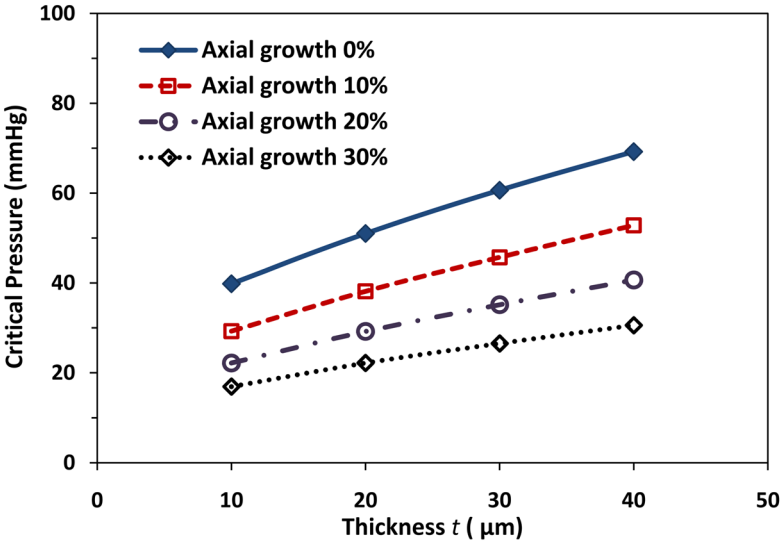

(a)

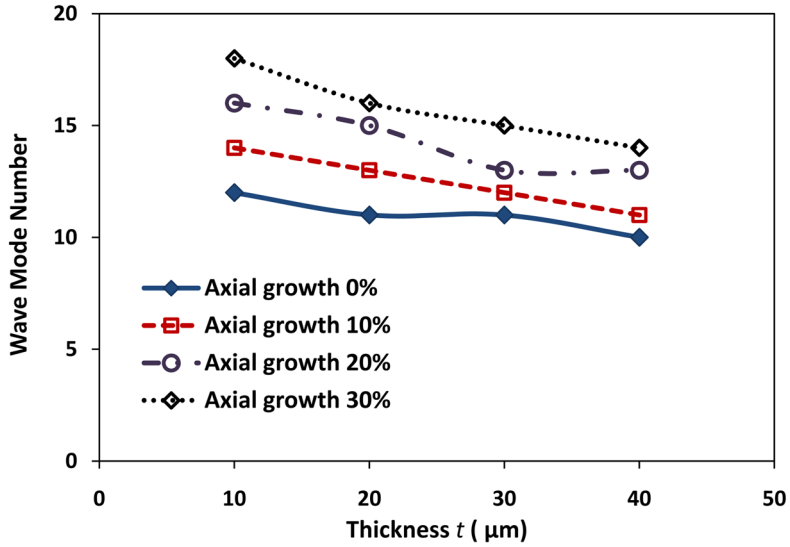

(b)

Figure 3.
Critical buckling pressure (a) and buckling mode (b) plotted as functions of wall thickness with constant lumen radius (R_i = 100 μm). Arteriole length l = 10 mm and k_s = 5 kPa.

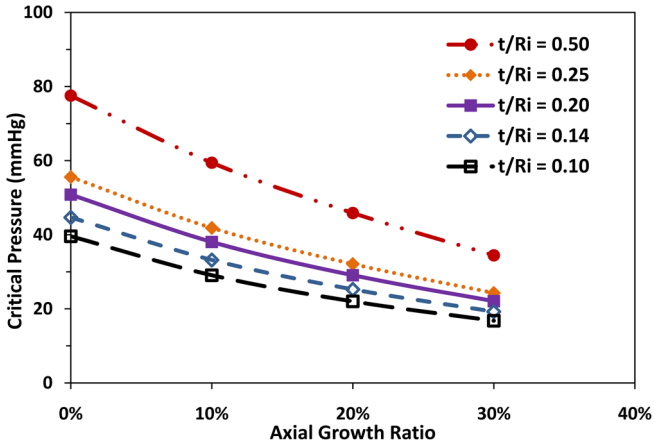

(a)

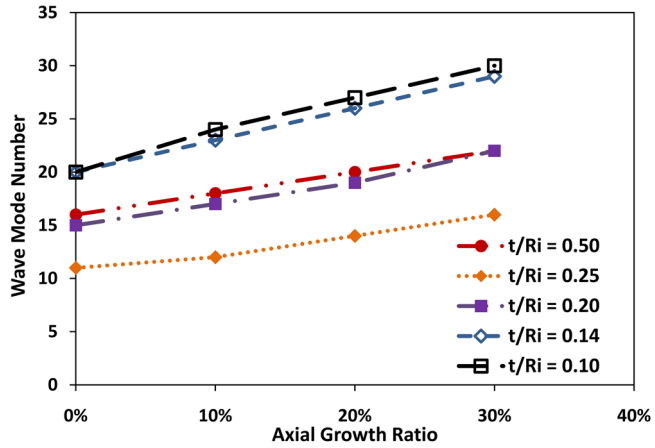

(b)

Figure 4.

comparison of critical buckling pressure (a) and buckling mode (b) plotted as functions of axial growth ratio at different t/R_i ratios. Arteriole R_i, t, and l were 50 μm, 10 μm, and 10 mm respectively, and k_s = 5 kPa.

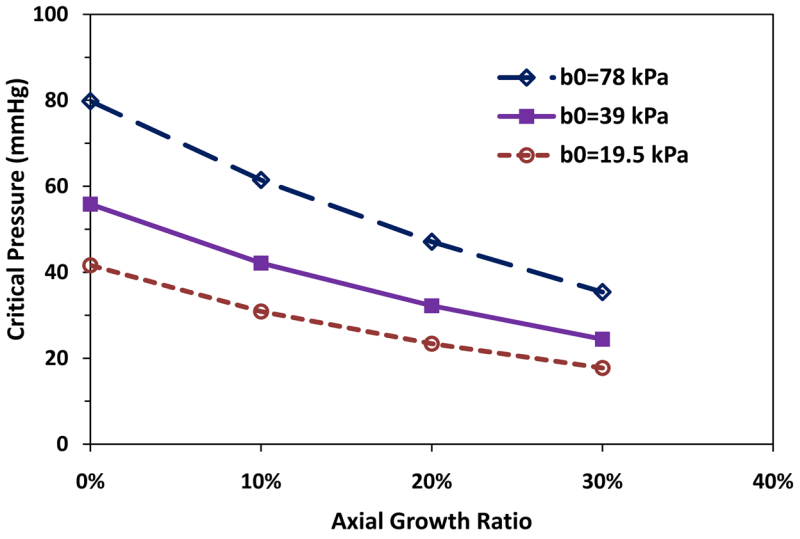

(a)

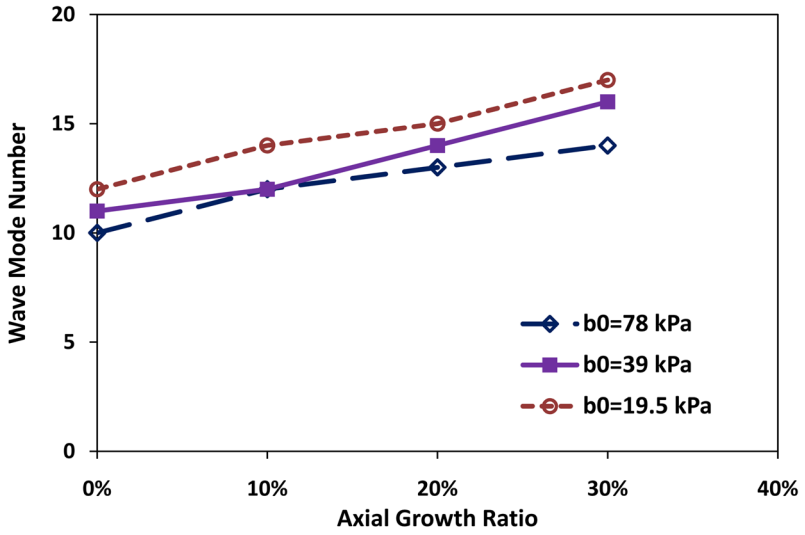

(b)

Figure 5.
Comparison of critical buckling pressure (a) and buckling mode (b) plotted as functions of axial growth ratio at different arterial wall material properties (b_0). Arteriole R, t, and l were 50 μm, 10 μm, and 10 mm respectively, and k_s = 5 kPa.

Table 1

Arteriolar buckling modes under axial and radial growth, initial radius $R_i = 50$ μm, $R_e = 60$ μm and length L=10 mm

Lumen Radius Growth Ratio	Final Dimension				Buckling Mode Number			
	Lumen R_i (μm)	Outer R_e (μm)	t/R_i	Remodeling Type	Axial growth ratio			
					0%	10%	20%	30%
1.2	60	90	0.50	hypertrophic	16	18	20	22
1.5	75	90	0.20	hypertrophic	15	17	19	22
2	100	125	0.25	hypertrophic	11	12	14	16
1.2	60	68.6	0.14	eutrophic	20	23	26	29
1.2	60	66	0.10	hypotrophic	20	24	27	30